

# Lawrence Berkeley National Laboratory

## Lawrence Berkeley National Laboratory

### **Title**

Exposing the non-collectivity in elliptic flow

### **Permalink**

<https://escholarship.org/uc/item/40j8b55h>

### **Author**

Koch, Volker

### **Publication Date**

2009-09-09

Peer reviewed

# Exposing the non-collectivity in elliptic flow

Jinfeng Liao\* and Volker Koch†

*Nuclear Science Division, Lawrence Berkeley National Laboratory,  
MS70R0319, 1 Cyclotron Road, Berkeley, CA 94720*

## Abstract

We show that backward-forward elliptic asymmetry correlations provide an experimentally accessible observable which distinguishes between collective and non-collective contributions to the observed elliptic asymmetry  $v_2$  in relativistic heavy ion collisions. The measurement of this observable will reveal the momentum scale at which collective expansion seizes and where the elliptic asymmetry is dominated by (semi)-hard processes. In addition, the knowledge of the actual magnitude of the collective component of the elliptic asymmetry will be essential for the extraction of the viscosity of the matter created in these collisions.

PACS numbers: 25.75.-q , 12.38.Mh

arXiv:0902.2377v1 [nucl-th] 13 Feb 2009

---

\* jliao@lbl.gov

† vkoch@lbl.gov

**Introduction.** — Deconfined QCD matter at high energy density, the so-called Quark-Gluon Plasma (QGP), was a phase during the evolution of the early universe and it is now created and explored experimentally in relativistic heavy ion collisions. One major discovery by the experimental program [1] of the Relativistic Heavy Ion Collider (RHIC) is the large elliptic asymmetry,  $v_2$ , of observed particles' transverse momenta, which is consistent with predictions from ideal hydrodynamic expansion. This led to the conjecture that the matter created in the collisions exhibits “perfect fluidity”, i.e. that its shear viscosity is very small. First studies [2, 3, 4, 5] indicate that the shear viscosity, usually presented as the viscosity over entropy density  $\eta/s$ , must be very small especially near  $T_c$ , much smaller than any known condensed matter substances and rather close to the conjectured universal lower bound  $\frac{\eta}{s} \geq \frac{1}{4\pi}$  based on calculations [6] utilizing the gauge/string duality.

The dependence on transverse momentum ( $p_t$ ) of the elliptic asymmetry  $v_2$ , as depicted in Fig. 1 shows a rise at low  $p_t$  towards a maximum at  $p_t \simeq 3 \text{ GeV}$ , and a constant value for large transverse momenta. The present understanding of this behavior is that the low  $p_t$  region,  $p_t \lesssim 1.5 \text{ GeV}$ , where the bulk of the matter is located, is due to *collective* hydrodynamic expansion: The initial spatial azimuthal asymmetry of created matter translates into a difference in pressure gradients and, thus, expansion rates along different directions, eventually leading to the observed  $v_2$  in transverse momentum space which extends widely along (pseudo)rapidity. The success of ideal hydrodynamic calculations [7] suggests that the QGP at temperatures around  $1 - 2T_c$  is indeed a strongly coupled system (sQGP) [8] with a remarkably small viscosity, which may be related to the mechanism of how QCD confinement occurs close to the transition point[9].

At very high transverse momenta, on the other hand,  $v_2$  is believed to be due to the different attenuation of hard partons (jet quenching) in the asymmetrically distributed matter [10, 11, 12]. In this case the elliptic asymmetry,  $v_2$ , is *non-collective* in the sense that it is due to rather local processes associated with the jet that is very narrowly distributed in rapidity. The transition from collective (hydrodynamic) to non-collective (jet-like) asymmetries is expected to take place at intermediate transverse momenta  $p_t \simeq 2 - 4 \text{ GeV}$ , but the details are not very well understood. In addition, one would think that the attenuation of the jets should result in local, non-collective asymmetries, also at lower transverse momenta, since the debris from the jet-quenching process need to go somewhere.

If, however, there is a sizeable non-collective contribution to  $v_2$  at low  $p_t$  the comparison

of (viscous) hydrodynamic calculations to the data may lead to wrong conclusions about the viscosity of the produced matter in these collisions. Therefore, it would be desirable to have a direct measurement not only of the transverse momentum at which the transition from collective to non-collective  $v_2$  occurs, but also of the contribution of non-collective effects in the region of low transverse momenta,  $p_t < 1.5$  GeV.

It is the purpose of this work to develop such an observable which will distinguish between the collective and the non-collective contributions to the elliptic asymmetry, by studying the appropriate correlations and fluctuations[13, 14, 15]. In the present work we will identify the collective component with hydrodynamic flow and the non-collective one with attenuated jets. This is solely for purpose of illustration and we note, that there may be other mechanisms at work which generate collective and/or non-collective components, which the observable proposed here is not able to disentangle from the commonly accepted mechanisms of hydrodynamic flow and jet quenching.

The key observation is the following: Consider two rapidity bins, one forward, one backward, with suitable separation (gap) in between. In a given event, the elliptic asymmetry of the collective component in both rapidity bins is highly correlated. The non-collective component, on the other hand, generates an elliptic asymmetry in either the forward bin or the backward bin, but never in both, resulting in very small backward-forward correlations. To illustrate this point, consider hydrodynamic expansion as an example for the collective component. In each event the elliptic asymmetry is aligned in azimuth and of comparable magnitude in the forward and backward rapidity bin. Actually most of the hydrodynamic calculations assume boost invariance implying infinite range rapidity correlations. Contrast this with the elliptic asymmetry due to quenched jets, as a example for a non-collective component. At RHIC energies one rarely has more than one hard process observed per event, and thus the asymmetry due to attenuated jets, for example the soft debris due to jet attenuation, will be local in rapidity and hence will not contribute to the long-range backward-forward correlation of the elliptic asymmetry. We note, that this situation will change at higher energies, such as the LHC, were we have many hard processes per event. In this case one may still consider a possible non-correlation at a rapidity separation that is larger than typical jet cone extension but smaller than average jet-jet separation. Based on the above, we will implement in the rest of this paper an experimentally measurable observable by correlating the backward-forward elliptic asymmetry and demonstrate how it

can diagnose the extent of collectivity in  $v_2$ .

**The correlation of elliptic asymmetry.**—Before going to the correlation of elliptic asymmetry, let us first briefly discuss  $v_2$  itself, defined as:

$$\langle v_2(p_t) \rangle = \frac{\int_0^{2\pi} d\phi \cos(2\phi) \langle \frac{d^2 N}{p_t dp_t d\phi} \rangle}{\int_0^{2\pi} d\phi \langle \frac{d^2 N}{p_t dp_t d\phi} \rangle} \quad (1)$$

In the above  $\langle \frac{d^2 N}{p_t dp_t d\phi} \rangle$  is the distribution of the event-averaged  $p_t$ -differential yield over the azimuthal angle  $\phi$  which is defined with respect to the reaction plane. [Throughout the paper we use  $\langle \rangle$  to denote average over collision events.] The numerator may be referred to as the total elliptic asymmetry of selected bin, which we will denote by  $V_2$ . The particle yield at RHIC can be attributed to two main sources: the bulk matter which dominates low  $p_t$  regime and exhibits collective flow, and the (partially suppressed) hard jets dominant at high  $p_t$ . Both sources contribute additively to the total yield  $\frac{d^2 N}{p_t dp_t d\phi}$  and thus to the measured  $v_2$ .

The proposed new observable is the correlation of the *total*  $V_2(p_t)$  in the two rapidity (backward-forward) bins. We may take the right slice  $y \in [y_{min}, y_{max}]$  and the left slice  $y \in [-y_{max}, -y_{min}]$  with  $0 < y_{min} < y_{max}$  which should be carefully selected experimentally: the rapidity gap  $(-y_{min}, y_{min})$  should be just large enough such that a fragmenting jet won't spread simultaneously into both bins, and  $y_{max}$  should be as large as possible but remain in the “flat plateau” near mid-rapidity. Specifically, we define the correlation  $\mathcal{C}_{LR}$  as:

$$\mathcal{C}_{LR}[p_T] \equiv \frac{\langle V_2^L \cdot V_2^R \rangle}{\langle V_2^L \rangle \cdot \langle V_2^R \rangle} \quad (2)$$

The  $V_2^L$  and  $V_2^R$  in the above are the total elliptic asymmetry in the respective rapidity bins (and  $p_t$  bin as well), i.e.

$$\langle V_2^{L/R}(p_t) \rangle = \int_0^{2\pi} d\phi \cos(2\phi) \left\langle \frac{dN^{L/R}}{d\phi} \right\rangle \quad (3)$$

$$\langle V_2^L \cdot V_2^R(p_t) \rangle = \left\langle \left[ \int_0^{2\pi} d\phi \cos(2\phi) \frac{dN^L}{d\phi} \right] \cdot \left[ \int_0^{2\pi} d\phi' \cos(2\phi') \frac{dN^R}{d\phi'} \right] \right\rangle \quad (4)$$

In the above we denote by  $\frac{dN^{L/R}}{d\phi}$  the  $\phi$ -differential particle yield in the  $L/R$  bins respectively. We emphasize these yields (and throughout the rest of the paper) are still  $p_t$ -dependent and their precise meaning is  $\frac{dN}{d\phi} \Big|_{p_t} \equiv \frac{dN}{p_t dp_t d\phi} \cdot p_t \cdot \Delta p_t$ .

We further introduce the combined distribution in the  $L + R$  bins  $\frac{dN^{L+R}}{d\phi} = \frac{dN^L}{d\phi} + \frac{dN^R}{d\phi}$ . The total yield in the full acceptance  $L + R$  can be decomposed into two components[11] — the hydro flow yield and the jets-related yield respectively:

$$\frac{dN^{L+R}}{d\phi} = \frac{dN^{\mathcal{F}}}{d\phi} \Big|_{L+R} + \frac{dN^{\mathcal{J}}}{d\phi} \Big|_{L+R} \quad (5)$$

(In the following we drop the  $L + R$  subscript.)

To quantify the main point, we can express the separate yields in  $L/R$  bins as:

$$\frac{dN^L}{d\phi} = \left(\frac{1}{2} + \eta^L\right) \cdot \left\langle \frac{dN^{\mathcal{F}}}{d\phi} \right\rangle + \xi \cdot \frac{dN^{\mathcal{J}}}{d\phi} \quad (6)$$

$$\frac{dN^R}{d\phi} = \left(\frac{1}{2} + \eta^R\right) \cdot \left\langle \frac{dN^{\mathcal{F}}}{d\phi} \right\rangle + (1 - \xi) \cdot \frac{dN^{\mathcal{J}}}{d\phi} \quad (7)$$

In the above we have introduced three random variables to schematically describe the fluctuations from event to event.  $\eta^{L/R}$  represent (independent) small random deviations from the average hydro flow yield in L/R bins, and satisfy  $\langle \eta^{L/R} \rangle = 0, \langle \eta^L \cdot \eta^R \rangle = 0$ . The variable  $\xi$  assumes values of either 0 or 1 in each event with equal probability, i.e.  $\langle \xi \rangle = \langle 1 - \xi \rangle = 1/2$  while  $\xi(1 - \xi) = 0$  holds in each event. The physical idea is that in each event there is at most one high  $p_t$  hadron cluster contributing to the final observed yield[16], which is located either in the left or the right rapidity slice. In contrast, the collective hydro flow (no matter perfect or viscous) contribution is about equally split between L/R.

Next we introduce an event-averaged  $\phi$ -integrated interpolation function:

$$g(p_t) = \frac{\int_0^{2\pi} d\phi \langle \frac{dN^{\mathcal{J}}}{d\phi} \rangle}{\int_0^{2\pi} d\phi \langle \frac{dN^{\mathcal{F}}}{d\phi} \rangle + \int_0^{2\pi} d\phi \langle \frac{dN^{\mathcal{J}}}{d\phi} \rangle} \quad (8)$$

with  $g(p_t)$  and  $1 - g(p_t)$  giving the relative weight of the jet (non-collective) and flow (collective) contribution to the total  $L + R$  yield, respectively. With this function we then calculate the actual observed  $\langle v_2 \rangle$  in  $L + R$  bin via (1) using the combined yield of both flow and jet:

$$\begin{aligned} \langle v_2(p_t) \rangle &= \frac{\int_0^{2\pi} d\phi \cos(2\phi) \left[ \langle \frac{dN^{\mathcal{F}}}{d\phi} \rangle + \langle \frac{dN^{\mathcal{J}}}{d\phi} \rangle \right]}{\int_0^{2\pi} d\phi \left[ \langle \frac{dN^{\mathcal{F}}}{d\phi} \rangle + \langle \frac{dN^{\mathcal{J}}}{d\phi} \rangle \right]} \\ &= [1 - g(p_t)] \cdot \langle v_2 \rangle^{\mathcal{F}} + g(p_t) \cdot \langle v_2 \rangle^{\mathcal{J}} \end{aligned} \quad (9)$$

In the above the  $\langle v_2^{\mathcal{F}/\mathcal{J}} \rangle$  are defined as in (1) with the corresponding hydro-flow-only/jet-only yields.

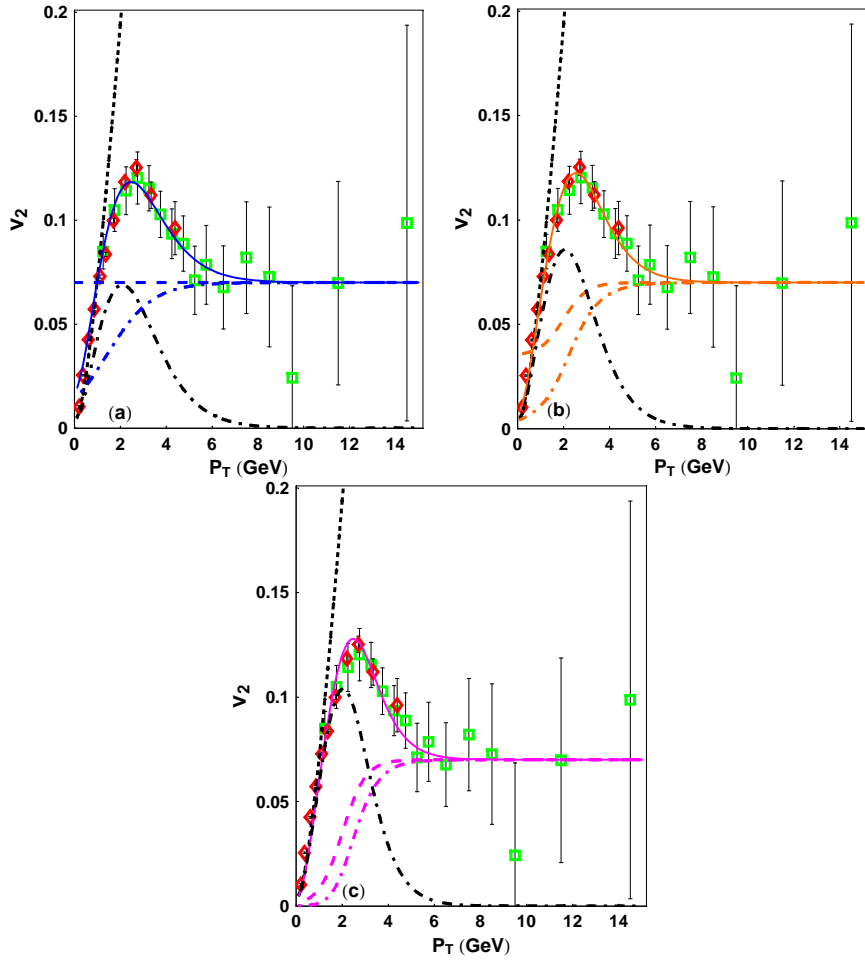


FIG. 1: Parametrization of AuAu 200 GeV  $v_2$  data (00-20% centrality bin). The red diamonds at low  $p_t$  are  $v_2$  for negative charged hadrons from [17] and the green boxes extending from 1.25 – 14.5 GeV are  $v_2$  for  $\pi_0$  from PHENIX run-7 preliminary [18]. The blue/orange/magenta solid lines in (a)/(b)/(c) represent the combined parametrization, Eq.(9), respectively. In all three panels, the black short-dashed lines at the left show the collective-flow-only contribution (calculated from the blast wave model) while the colored long-dashed lines (horizontally extending to very high  $p_t$ ) show the jet-only contribution in Eq.(13). The dash-dotted lines show the weighted contribution from the hydro flow  $(1 - g) \cdot \langle v_2^{\mathcal{F}} \rangle$  (black) and from the jet  $g \cdot \langle v_2^{\mathcal{J}} \rangle$  (colored), respectively. (See text for more details.)

Combining (6,7,8,9) with (3,4) and using the formulae for fluctuation/correlation in [15], the evaluation of (2) gives the following final result:

$$\mathcal{C}_{LR} = \frac{(1 - g)^2 [\langle v_2 \rangle^{\mathcal{F}}]^2 + 2g(1 - g) [\langle v_2 \rangle^{\mathcal{F}} \cdot \langle v_2 \rangle^{\mathcal{J}}]}{[(1 - g) \langle v_2 \rangle^{\mathcal{F}} + g \langle v_2 \rangle^{\mathcal{J}}]^2} \quad (10)$$

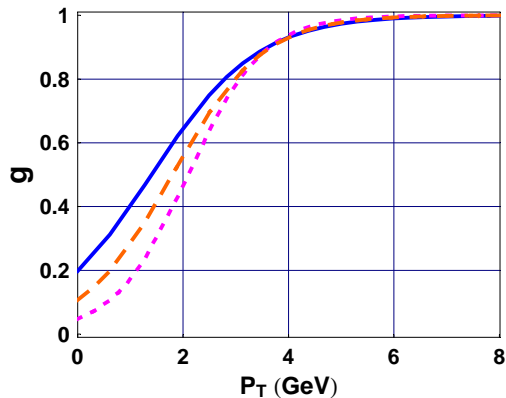


FIG. 2: The interpolation function  $g(p_t)$  defined by Eq.(14) as a measure of non-collectivity. The solid blue line is obtained for case (a) in Eq.(13), orange long-dashed line for case (b), and magenta short-dashed line for case (c).

A distinct feature is that as  $g \rightarrow 0$  (hydro flow dominance) one finds  $\mathcal{C}_{LR} \rightarrow 1$  while  $\mathcal{C}_{LR} \rightarrow 0$  in the other limit  $g \rightarrow 1$  (jet dominance): thus this correlation  $\mathcal{C}_{LR}[p_t]$  can distinguish the collective/non-collective contributions and expose the transition from collective flow to jet regime. To further evaluate it, we need a suitable parametrization of the hydro flow and jet contributions.

**Calculation of  $\mathcal{C}_{LR}$ .**—We first deal with hydro flow and jet yields separately and then use the interpolation function (8) to combine them. To be specific, in the rest of this paper we will focus on the PHENIX  $v_2$  data[16, 17, 18] for AuAu 0 – 20% centrality class at  $\sqrt{s} = 200$  GeV as experimental input (see Fig.1), which extends from low  $p_t$  all the way to 14.5 GeV.

For the hydro flow yield, a convenient approximation to describe this collective part is the blast-wave model (see e.g. [19]) which parameterizes the final velocity field of the flow at freeze-out (with Cooper-Frye procedure) to calculate observables like  $v_2$ . For simplicity we follow the approach of [19], i.e.:

$$\left\langle \frac{dN^{\mathcal{F}}}{d\phi} \right\rangle \propto \frac{1}{(2\pi)^3} \int \frac{p^\mu d\sigma_\mu}{e^{p^\mu u_\mu / T_o} - 1} \quad (11)$$

The elliptic flow is intrinsically built in the flow field  $u^\mu(x^\mu)$ : in  $(\tau, \eta_s, r, \phi_s)$  coordinates  $u^r = \frac{r}{R} u_o [1 + u_2 \cos(2\phi_s)] \Theta(R_o - r)$ ,  $u^\tau = \sqrt{1 + (u^r)^2}$ ,  $u^{\phi_s} = u^{\eta_s} = 0$ . The integration measure at freeze-out  $\tau_o$  is  $p^\mu d\sigma_\mu = m_T \cosh(y - \eta_s) \tau_o d\eta_s r dr d\phi_s$ . The blast-wave parameters are chosen as  $m_\pi = 140$  MeV,  $T_o = 170$  MeV,  $R_o = 10$  fm,  $\tau_o = 7$  fm,  $u_o = 0.7$ , and  $u_2 = 0.06$



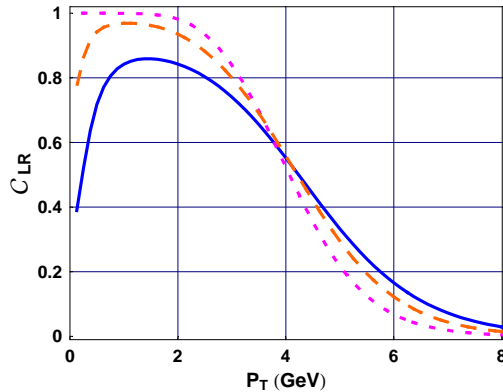


FIG. 3: The correlation  $\mathcal{C}_{LR}(p_t)$ . The solid blue line is calculated for case (a) in Eq.(13), the orange long-dashed line for case (b), and the magenta short-dashed line for case (c).

in order to approximately reproduce the measured yield at low  $p_t$  (see Table.XIV in [16]). We refer the readers to [19] (section V and Appendix A) for more details regarding the blast-wave model. Within this model one can numerically calculate the flow-only  $\langle v_2^{\mathcal{F}} \rangle$  via (1) using the flow yield (11) (black short-dashed lines in Fig.1(a,b,c)). We also show the weighted flow contribution  $(1-g) \cdot \langle v_2^{\mathcal{F}} \rangle$  as the black dash-dot lines.

The jet-related production, on the other hand, can be parameterized as

$$\left\langle \frac{dN^{\mathcal{J}}}{d\phi} \right\rangle \propto \frac{1}{(1 + p_t/P_0)^n} \left[ 1 + 2 \langle v_2^{\mathcal{J}} \rangle \cdot \cos(2\phi) \right] \quad (12)$$

The above parametrization reflects the asymmetric jet attenuation along different directions which causes a considerable azimuthal asymmetry in high  $p_t$  yield as parameterized by  $\langle v_2^{\mathcal{J}} \rangle [p_t]$ . While the experimental data indicate  $\langle v_2^{\mathcal{J}} \rangle [p_t]$  to be quite sizeable (7%) and rather *constant* for  $p_t > 6$  GeV [18], it is not clear how  $v_2^{\mathcal{J}}$  behaves at lower  $p_t$ . To explore this we, therefore, use three possible parameterizations (with  $p_t$  in GeV)

$$\begin{aligned} (a) \quad & \langle v_2^{\mathcal{J}} \rangle = 0.07 \\ (b) \quad & \langle v_2^{\mathcal{J}} \rangle = 0.07 \cdot \left[ \frac{3}{4} + \frac{1}{4} \tanh(p_t - 2) \right] \\ (c) \quad & \langle v_2^{\mathcal{J}} \rangle = 0.07 \cdot \left[ \frac{1}{2} + \frac{1}{2} \tanh(p_t - 4) \right] \end{aligned} \quad (13)$$

The three cases feature different patterns for the jet contribution to  $v_2$  at low  $p_t$ , which are shown as colored long-dashed lines in Fig.1 correspondingly, with the weighted jet contributions  $g \cdot \langle v_2^{\mathcal{J}} \rangle$  shown as colored dash-dot lines.

To combine the hydro flow and jet contributions requires the interpolation function (8), which we parameterize as:

$$g(p_t) = \frac{1}{2} [1 + \tanh[(p_t - P_C)/P_W]] \quad (14)$$

The parameters  $P_C, P_W$  can be determined by  $\chi^2$  fitting of the currently available  $v_2(p_t)$  data. We find that the best choices for the three cases to be: case (a)  $P_C = 1.4$  GeV and  $P_W = 2$  GeV; (b)  $P_C = 2.4$  GeV and  $P_W = 1.8$  GeV; (c)  $P_C = 2.4$  GeV and  $P_W = 1.8$  GeV. In all cases a reasonable model description of the  $v_2$  data is established over the whole  $p_t$  range, as can be seen in Fig.1. In Fig.2 we plot  $g(p_t)$  for the three cases: solid blue solid line for (a), orange short-dashed line for (b), and magenta long-dashed line for (c). One sees that they differ considerably in the amount of non-collective component at low to intermediate  $p_t$ . Of course the plotted curves only schematically demonstrate what may happen. To quantify the  $g(p_t)$  much more experimental information will be required. As a side remark, the admixture of a smaller jet  $v_2$  seems to be a natural and plausible alternative scenario to viscous corrections for a reduced  $v_2$  at low transverse momenta.

Finally given the above parametrization we can calculate the proposed correlation  $\mathcal{C}_{LR}$  using (10). The results are shown in Fig.3: the solid blue line is for case (a), the orange short-dashed line for case (b), and the magenta long-dashed line for case (c). While all three cases produce similar  $v_2$ , they are readily distinguishable by  $\mathcal{C}_{LR}$  from low to intermediate  $p_t$  region. The non-monotonic structure seen in cases (a) and (b) is due to interplay between a *non-vanishing* jet contribution and rapidly rising hydro flow contribution to  $v_2$  at low  $p_t$ , which is absent in case (c). From the distinct deviations of  $\mathcal{C}_{LR}$  from unity it can be deduced how much the non-collective component contributes at low  $p_t$  and how it grows with increasing  $p_t$ . While the curves in Fig.3 depend on the specific parametrization, they demonstrate the sensitivity of  $\mathcal{C}_{LR}$  to the non-collectivity which may hide in the elliptic asymmetry  $v_2$ .

**Summary and discussion.**— In summary, we have proposed to use the correlation of  $V_2$  as defined in (2) to distinguish the collective (hydro-flow) from non-collective (jet) contributions to  $v_2$ . Using a suitable two-component parametrization, we have studied the sensitivity of this observable to the degree of non-collectivity. We have further demonstrated that this observable is capable of exposing the transition from hydro flow to jet with increasing  $p_t$ .

As always, there are “real world” complications regarding practical measurements of the correlation. One issue is that even though the asymmetry of the hydro flow field is perfectly aligned in the L/R bins, the actually produced particles in the two bins may deviate (both in magnitude and in orientation) from the supposed “ $v_2$ ” due to statistical fluctuation (see an elegant discussion in [20]). This will reduce the correlation from unity even for purely hydro flow, with the effect scaling as  $1/\sqrt{N_{bin}}$ . The other issue relates to the low number of particles in each event from intermediate to high  $p_t$  which may cause the correlation to vanish trivially. These problems may be partially cured by selecting an appropriate size of the  $p_t$  bin and/or event trigger. Also those effects are small at low  $p_t$  region, where the particle abundance is large.

The study presented here is intended to motivate a dedicated experimental investigation of the proposed correlation. As we suggest, experimental data for  $\mathcal{C}_{LR}$ , when becoming available, will reveal the magnitude of the collective contribution to  $v_2$  and the transition pattern of  $v_2$  between collective and non-collective behavior. It would also be very interesting to see how the pattern will change with centrality, as the hydro flow and jet components scale differently with collision centrality. In addition, these measurements will help to understand the origin of the decreasing  $v_2$  at intermediate  $p_t$  and will constrain viscous hydro corrections as well.

**Acknowledgements:** We would like to thank Mateusz Ploskon for helpful discussions concerning the experimental aspects of the proposed observable. The work is supported by the Director, Office of Energy Research, Office of High Energy and Nuclear Physics, Divisions of Nuclear Physics, of the U.S. Department of Energy under Contract No. DE-AC02-05CH11231.

- 
- [1] J. Adams *et al.* [STAR Collaboration], Nucl. Phys. A **757**, 102 (2005). K. Adcox *et al.* [PHENIX Collaboration], Nucl. Phys. A **757**, 184 (2005). I. Arsene *et al.* [BRAHMS Collaboration], Nucl. Phys. A **757**, 1 (2005). B. B. Back *et al.*, Nucl. Phys. A **757**, 28 (2005).
  - [2] L. P. Csernai, J. I. Kapusta and L. D. McLerran, Phys. Rev. Lett. **97**, 152303 (2006).
  - [3] R. A. Lacey *et al.*, Phys. Rev. Lett. **98**, 092301 (2007)
  - [4] P. Romatschke and U. Romatschke, Phys. Rev. Lett. **99**, 172301 (2007); H. Song and

- U. W. Heinz, Phys. Lett. B **658**, 279 (2008); K. Dusling and D. Teaney, Phys. Rev. C **77**, 034905 (2008).
- [5] H. B. Meyer, Phys. Rev. D **76**, 101701 (2007).
- [6] G. Policastro, D. T. Son and A. O. Starinets, Phys. Rev. Lett. **87**, 081601 (2001); P. Kovtun, D. T. Son and A. O. Starinets, Phys. Rev. Lett. **94**, 111601 (2005).
- [7] D. Teaney, J. Lauret and E. V. Shuryak, Phys. Rev. Lett. **86**, 4783 (2001); arXiv:nucl-th/01110037. P. F. Kolb, P. Huovinen, U. W. Heinz and H. Heiselberg, Phys. Lett. B **500**, 232 (2001); P. F. Kolb, J. Sollfrank and U. W. Heinz, Phys. Rev. C **62**, 054909 (2000).
- [8] M. Gyulassy and L. McLerran, Nucl. Phys. A **750**, 30 (2005). E. V. Shuryak, Nucl. Phys. A **750**, 64 (2005); Prog. Part. Nucl. Phys. **53**, 273 (2004); Prog. Part. Nucl. Phys. **62**, 48 (2009).
- [9] J. Liao and E. Shuryak, Phys. Rev. C **75**, 054907 (2007); Phys. Rev. Lett. **101**, 162302 (2008); Phys. Rev. D **73**, 014509 (2006). M. N. Chernodub and V. I. Zakharov, Phys. Rev. Lett. **98**, 082002 (2007). A. D'Alessandro and M. D'Elia, Nucl. Phys. B **799**, 241 (2008). C. Ratti and E. Shuryak, arXiv:0811.4174 [hep-ph].
- [10] E. V. Shuryak, Phys. Rev. C **66**, 027902 (2002); A. Drees, H. Feng and J. Jia, Phys. Rev. C **71**, 034909 (2005).
- [11] M. Gyulassy, I. Vitev and X. N. Wang, Phys. Rev. Lett. **86**, 2537 (2001). X. N. Wang, Phys. Rev. C **63**, 054902 (2001)
- [12] J. Liao and E. Shuryak, arXiv:0810.4116 [nucl-th].
- [13] S. Jeon and V. Koch, Phys. Rev. Lett. **83**, 5435 (1999); Phys. Rev. Lett. **85**, 2076 (2000).
- [14] V. Koch, A. Majumder and J. Randrup, Phys. Rev. Lett. **95**, 182301 (2005).
- [15] S. Jeon and V. Koch, arXiv:hep-ph/0304012; V. Koch, arXiv:0810.2520 [nucl-th].
- [16] S. S. Adler *et al.* [PHENIX Collaboration], Phys. Rev. C **76**, 034904 (2007).
- [17] S. S. Adler *et al.* [PHENIX Collaboration], Phys. Rev. Lett. **91**, 182301 (2003).
- [18] See e.g. Carla M Vale, "High  $p_T$  results from PHENIX", talk at Hard Probe 2008.
- [19] D. Teaney, Phys. Rev. C **68**, 034913 (2003).
- [20] J. Y. Ollitrault, Phys. Rev. D **48**, 1132 (1993).